

A Sparse Tensor Generator with Efficient Feature Extraction

TUGBA TORUN, EREN YENIGUL, AMEER Taweel, and DIDEM UNAT, Koç University, Turkey

Sparse tensor operations are gaining attention in emerging applications such as social networks, deep learning, diagnosis, crime, and review analysis. However, a major obstacle for research in sparse tensor operations is the deficiency of a broad-scale sparse tensor dataset. Another challenge in sparse tensor operations is examining the sparse tensor features, which are not only important for revealing its nonzero pattern but also have a significant impact on determining the best-suited storage format, the decomposition algorithm, and the reordering methods. However, due to the large sizes of real tensors, even extracting these features becomes costly without caution. To address these gaps in the literature, we have developed a smart sparse tensor generator that mimics the substantial features of real sparse tensors. Moreover, we propose various methods for efficiently extracting an extensive set of features for sparse tensors. The effectiveness of our generator is validated through the quality of features and the performance of decomposition in the generated tensors. Both the sparse tensor feature extractor and the tensor generator are open source with all the artifacts available at <https://github.com/sparcityeu/feaTen> and <https://github.com/sparcityeu/genTen>, respectively.

Additional Key Words and Phrases: sparse tensors, feature extraction, synthetic data generation

1 INTRODUCTION

Several applications such as social networks, deep learning, diagnosis, crime, and review analysis require the data to be processed in the form of multi-dimensional arrays, namely *tensors* [2, 13, 18, 19, 25, 34]. Tensors are extensions of matrices that can have three or more dimensions, or so-called *modes*. Tensor decomposition techniques such as CPD and Tucker are widely used to analyze and reveal the latent features of such real-world data in the form of sparse tensors [10, 16]. For making the tensor decomposition methods faster or more memory-efficient, numerous storage formats and partitioning or reordering schemes are introduced in the literature [3, 11, 14, 21, 22, 27]. However, the performance of these schemes highly depends on the sparsity pattern of the tensor.

Efficiently extracting the sparsity pattern of a given tensor is essential for optimizing various aspects of tensor analysis and manipulation. The structural features can inform format selection, aiding in determining the most suitable storage format. It can influence the algorithm selection, with different tensor operations exhibiting varying performance based on the sparsity characteristics. Understanding the sparsity pattern also provides insights into the performance of decomposition techniques. In a recent work, [33], some tensor features are used to automatically predict the best storage format for a sparse tensor via machine learning techniques. However, the work considers the features for only a single mode, which may cause lack of some critical intuition from other dimensions.

Sparse tensors in real-world scenarios often exhibit extreme sparsity, with densities as low as 10^{-15} . Unlike the sparse matrices often containing at least one nonzero in their rows and columns, sparse tensors contain numerous empty fibers and slices, which are one- and two-dimensional fragments of tensors. A naive approach for extracting sparse tensor features involves traversing the tensor nonzeros in coordinate (COO) format and updating the nonzeros of respective slices and fibers. However, this approach becomes impractical for large tensors with increasing dimensions. Another approach [33] is to assume that the tensor is already sorted to extract the features, yet it reveals the features from only a single mode order. Since the sizes of a sparse tensor diverge a lot along different modes, focusing the features solely on one perspective might lead to the loss of crucial structural information inherent in the tensor.

Authors' Contact Information: Tugba Torun, ttorun@ku.edu.tr; Eren Yenigul, eyenigul19@ku.edu.tr; Ameer Taweel, ataweel20@ku.edu.tr; Didem Unat, dunat@ku.edu.tr, Koç University, İstanbul, Turkey.

To tackle these challenges, we develop a sparse tensor feature extraction framework, FEATen, which extracts a detailed and exclusive set of sparse tensor features, encapsulating the features along all modes. It extends the feature set by including important size-independent features such as coefficient of variation and imbalance to gain a deeper insight into the nonzero distribution. Additionally, FEATen offers four alternative feature extraction methods for efficiency, providing flexibility to select the most suitable method based on machine and tensor characteristics.

By utilizing the generated features, machine learning tools can be used to reveal the most suitable storage format, partitioning, or reordering method that fits best with that tensor. Nevertheless, the primary challenge facing this research stems from the necessity of having thousands of samples to train machine learning models. Conversely, the majority of multi-dimensional real-world data require manual cleaning to become readily usable in research. Meanwhile, efforts to gather publicly available real-world data as sparse tensor collections yield only a few instances [12, 28]. Moreover, tensor sizes can be large, making it inconvenient to download, read, and use them in computation. A tensor generator for performance analysis purposes can be handy, enabling the study of algorithms by generating tensors on the fly and discarding them if necessary.

To fill these gaps in the literature, we propose a smart sparse tensor generator, GENTen, that takes the significant features of tensors into consideration. The proposed generator can be utilized to produce sparse tensors with features resembling those of real tensors, thereby forming a large suite of sparse tensor dataset. Moreover, an important benefit of this generator is its use of size-independent features like coefficient of variation, imbalance, and density, enabling easy generation of instances with different sizes, thereby enhancing its versatility across various contexts. The effectiveness of the generator is validated by comparing the features and CPD performance of the generated tensors with the naive random and the original real-world tensors.

The main contributions of this work are:

- A sparse tensor feature extraction framework, FEATen, is developed. It includes four different feature extraction methods, which can be used alternatively depending on the computation needs and the characteristics of input tensors. All methods in FEATen are parallelized using OpenMP.
- We develop a smart sparse tensor generator, GENTen, which considers significant tensor features. It can be used to generate an artificial tensor dataset in which the properties and characteristics of the generated tensors are similar to the real-world tensors. GENTen is parallelized with OpenMP for faster generation.
- Both tools are open source^{1 2}, accompanied by comprehensive documentation and illustrative examples tailored for the community's usage.

This manuscript is organized as follows. Section 2 provides the background information on sparse tensors and tensor decomposition. The proposed feature extraction tool is introduced in Section 3. In Section 4, we present our sparse tensor generator, GENTen. Experimental results are reported in Section 5. We discuss the related works in Section 6 and conclude in Section 7.

2 BACKGROUND

A tensor with M dimensions is called an M -mode or M th order tensor, where the mode count, M , is referred to as the order of tensor. Mode m of a tensor refers to its m th dimension. *Fibers* are defined as the one-dimensional sections of a tensor obtained by fixing all but one index. *Slices* are two-dimensional sections of a tensor obtained by fixing every

¹<https://github.com/sparcityeu/feaTen>

²<https://github.com/sparcityeu/genTen>

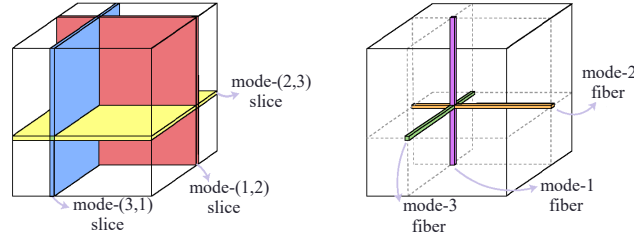


Fig. 1. Sample slice and fibers of a 3-mode tensor.

index but two. Figure 1 depicts sample slice and fibers of a 3-mode tensor. The numbers in the naming of slices and fibers derive from the mode indices that are not fixed while forming them. For instance, $X(i, :, :)$ is a mode-(2,3) slice, and $X(i, j, :)$ is a mode-3 fiber of a 3-mode tensor X , where a tensor element with indices i, j, k is denoted by $X(i, j, k)$. A fiber (slice) is said to be a *nonzero fiber (slice)* if it contains at least one nonzero element; and an *empty fiber (slice)*, otherwise.

To reveal the relationship of data across different modes, tensor decomposition techniques are widely used. Canonical Polyadic Decomposition (CPD) and Tucker decomposition are the most two popular ones among them. In Tucker decomposition, a tensor is decomposed into a much smaller core tensor and a set of matrices; whereas in CPD, a tensor is factorized as a set of rank-1 tensors, which can be considered as a generalization of matrix singular value decomposition (SVD) method for tensors.

There are various implementations for CPD and each has different storage schemes and reordering algorithms proposed specifically for that scheme. SPLATT [31] and ParTI [20] are the two most commonly-used libraries for CPD. ParTI is a parallel tensor infrastructure that supports essential sparse tensor operations and tensor decompositions on multicore CPU and GPU architectures. SPLATT provides a shared-memory implementation for CPD while adopting a medium-grain partitioning for sparse tensors for parallel execution of CPD.

3 FEATURE EXTRACTION

The features of a sparse tensor have the capacity to reveal the most suitable storage format, partitioning or reordering method that fits best with that tensor if well-examined. The main challenge in extracting the sparse tensor features is to determine which and how many fibers and slices are nonzero. This is because the real-world sparse tensors are highly sparse and contain many empty fibers and slices. One naive approach for sparse tensor feature extraction is to traverse the tensor nonzeros in coordinate (COO) format and update the number of nonzeros of the respective slices and fibers. However, this approach is not practical for large tensors since the real-world tensors often have huge numbers of fibers and slices. For instance, some real tensors have more than 10^{19} fibers, and even storing a boolean array of such a large size requires a space of 10 million Terabytes, which is impractical in modern machines (See the properties of some real tensors in Table 3). To overcome these challenges, we propose and implement four alternative methods for sparse tensor feature extraction.

3.1 Feature Set

We consider three *kinds* of statistics for sparse tensors: (i) nonzeros per nonzero slices, (ii) nonzeros per nonzero fibers, (iii) nonzero fibers per nonzero slices. Table 1 depicts the global features of the tensor that are independent of these

Table 1. Extracted global features of tensors.

Feature	Description	Formula
size_m	Size of tensor in mode m	I_m
nnz	Number of nonzeros	$\text{nz}(\mathcal{X})$
d _{nz}	Density of nonzeros	$\text{nz}(\mathcal{X}) / \prod I_m$
n _{fib} _{all}	Number of all fibers	$\sum \mathcal{F}_m $
n _{slc} _{all}	Number of all slices	$\sum S_{k,\ell} $
n _{fib} _{nz}	Number of nz fibers	$\sum \text{nz}(\mathcal{F}_m) $
n _{slc} _{nz}	Number of nz slices	$\sum \text{nz}(S_{k,\ell}) $
d _{fib}	Density of nz fibers	$\text{nfib}_{\text{nz}} / \text{nfib}_{\text{all}}$
d _{slc}	Density of nz slices	$\text{nslc}_{\text{nz}} / \text{nslc}_{\text{all}}$

Table 2. Mode- and kind- dependent features that are extracted for each mode and for each kind: (i) nonzeros per slice, (ii) nonzeros per fiber, (iii) fibers per slice.

Feature	Description	Formula
n _{all}	All count including empty	*
n _{nz}	Nonzero count	*
nz_density	Nonzero sparsity	$\text{n}_{\text{nz}} / \text{n}_{\text{all}}$
max	Maximum value	*
min	Minimum value	*
dev	Deviation	$\text{max} - \text{min}$
sum	Summation of values	*
avg _{all}	Average value	$\text{sum} / \text{n}_{\text{all}}$
imbal _{all}	Imbalance	$(\text{max} - \text{avg}_{\text{all}}) / \text{max}$
stDev _{all}	Standard deviation	*
cv _{all}	Coefficient of variation	$\text{stDev}_{\text{all}} / \text{avg}_{\text{all}}$
avg _{nz}	Average by excluding empty	$\text{sum} / \text{n}_{\text{nz}}$
imbal _{nz}	Imbalance by excluding empty	$(\text{max} - \text{avg}_{\text{nz}}) / \text{max}$
stDev _{nz}	stDev by excluding empty	*
cv _{nz}	cv by excluding empty	$\text{stDev}_{\text{nz}} / \text{avg}_{\text{nz}}$

*Omitted due to the complex or trivial formula.

kinds. Table 2 shows the mode- and kind-dependent features that we have extracted for all of these three kinds and for all modes. Here by referring to all modes, we mean all possible angles that a slice or fiber can have through fixing different modes. For example, mode-(1,2), mode-(2,3), and mode-(3,1) slices represent all modes for slices of a 3-mode tensor. For ease of expression, we refer to the set of slices (fibers) along different modes as *slice-modes* (*fiber-modes*).

A tensor \mathcal{X} of size $I_1 \times I_2 \times \dots \times I_M$ is assumed to be given as an input in Coordinate format, i.e. the extension of matrix-market format for tensors. In the formulas, $\text{nz}(\cdot)$ is used as a function returning the number of nonzeros. \mathcal{F}_m refers to the set of fibers in mode- m , whereas $S_{k,\ell}$ refers to the set of slices obtained by fixing indices in modes k and ℓ . In the feature names, \bullet_{nz} refers to considering only nonzero kind-entries in the computation, i.e. nonzero fibers or slices, by ignoring the empty fibers or slices. \bullet_{all} refers to considering all kind-entries in the computation, including the empty ones. For instance, for the nonzeros-per-fiber kind in mode 1, n_{all} gives the number of all mode-1 fibers including empty, whereas n_{nz} gives the number of only nonzero fibers along mode-1.

In addition to the tensor features utilized in the related work [33], we also include the features of load imbalance, standard deviation, and coefficient of variation. In [26], it is shown that a high standard deviation of fiber length causes inter-warp load imbalance and low occupancy; whereas high standard deviation of the slice volume is related to significant inter-thread-block load imbalance. The coefficient of variation is another commonly-used metric for analysis which allows to compare between data sets with widely different means. For example, it is used to evaluate the dispersion of the number of nonzero elements per row for sparse matrix computations [1].

3.2 Extraction Workflow

The feature extraction process consists of two main stages, namely *array construction* and the *final reduction* phases. In the array construction phase, we construct three arrays for all modes: (i) $n_{\text{slc}}^{\text{nz}}$ (number of nonzeros per slice), (ii) $n_{\text{fib}}^{\text{nz}}$ (number of nonzeros per fiber), (iii) $n_{\text{slc}}^{\text{fib}}$ (number of fibers per slice). Here and hereafter, only the nonzero slices and nonzero fibers are considered when referring to slices and fibers, if not stated otherwise. Then in the final reduction

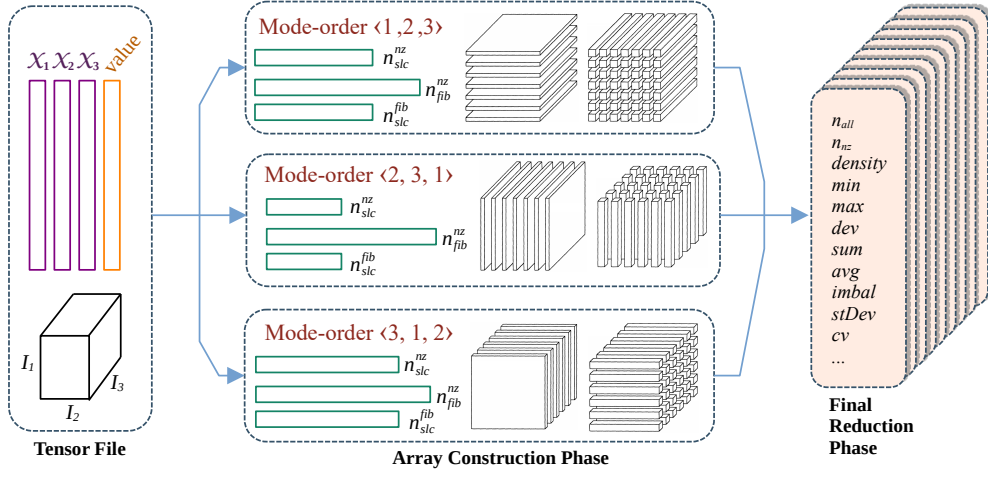


Fig. 2. The workflow of feature extraction for a 3-mode tensor using the mode-order approach.

phase, we extract all the sparse tensor features by traversing or applying a reduction on these smaller arrays. Both the array construction and the final reduction phases of FEATEN are parallelized using OpenMP.

The arrays of n_{slc}^{nz} and n_{slc}^{fib} are constructed for each slice-mode, so that there will be $\binom{M}{2}$ of them. The array n_{fib}^{nz} is constructed for each fiber-mode, hence yielding M different n_{fib}^{nz} arrays. For instance, for a 3-mode tensor, there are 3 different types of statistics for n_{slc}^{nz} and n_{slc}^{fib} which correspond to mode-(1,2), (2,3), and (3,1) slices; whereas for n_{fib}^{nz} , there are 3 different types of statistics corresponding to mode-1, 2, and 3 fibers. Since there are 11 global features and 15 mode- and kind-dependent features, the total number of features extracted for a 3-mode tensor is $15 \times 3 \times 3 + 11 = 146$ in total. For a 4-mode tensor, slices are along $\binom{4}{2} = 6$ different mode pairs, and fibers are along 4 different modes, so in total $15 \times 6 \times 2 + 15 \times 4 + 11 = 251$ features are considered. For 5-mode tensors, slices are along $\binom{5}{2} = 10$ different mode pairs, and fibers are along 5 different modes, yielding a total of $15 \times 10 \times 2 + 15 \times 5 + 11 = 386$ features.

One approach in FEATEN is to consider the slice and fiber modes in relation to mode execution orders. By saying *mode-order* $\langle i, j, k \rangle$, we can think that the COO-based index arrays of tensor \mathcal{X} are virtually rearranged to $\langle \mathcal{X}_i, \mathcal{X}_j, \mathcal{X}_k \rangle$ instead of the original order $\langle \mathcal{X}_1, \mathcal{X}_2, \mathcal{X}_3 \rangle$. In this context, we consider the slices are obtained by fixing all indices except the last two index, and the fibers are obtained by fixing all indices except the last one. For instance in mode order $\langle 1, 2, 3 \rangle$, we consider mode-(2,3) slices and mode-3 fibers. The advantage of this approach is to combine slices and fibers so that their corresponding computations may overlap.

Note that especially when computing n_{slc}^{fib} arrays, two different fiber modes can be associated with each slice mode. To be more specific, to extract the number of fibers per mode- (i, j) slices, it is possible to consider either mode- i or mode- j fibers. For this reason, to cover all slice and fiber modes, one can use both the mode-order set $\langle 1, 2, 3 \rangle, \langle 2, 3, 1 \rangle, \langle 3, 1, 2 \rangle$ or the mode-order set $\langle 1, 3, 2 \rangle, \langle 2, 1, 3 \rangle, \langle 3, 2, 1 \rangle$. Fig. 2 depicts the workflow of the feature extraction process for a 3-mode sparse tensor for the first case. In the final reduction phase, nine different sets of mode- and kind-dependent features are extracted in parallel, corresponding to three different versions of n_{slc}^{nz} , n_{fib}^{nz} , and n_{slc}^{fib} arrays from distinct mode-orders.

The mode-order approach is especially practical for 3-mode tensors. It is because the number of slice-modes and fiber-modes are both equal to three, making a one-to-one mapping possible between slice- and fiber-modes, hence

execution on three distinct mode-orders is sufficient to cover all cases. However for higher dimensions, it can cause some calculations for n_{fib}^{nz} to be repeated since the number of slice-modes becomes larger than the number of fiber-modes. Therefore we obey different approaches in different methods of FEATEN.

3.3 Extraction Methods

In order to overcome the memory and speed limitations in trivial feature extraction approaches, we propose four different feature extraction methods that can be used alternatively depending on the computation needs and the characteristics of input tensors. These methods are heap-based, sorting-based, grouping-based, which is first proposed in this work, and a hybrid method, which is a combination of sorting- and grouping-based methods.

Hash-based method: We implement a hash-table-based method to solve the memory issue of the COO-based naive method for large sparse tensors. Instead of long arrays that mostly contain zero values, we use a hash table that has keys as slice or fiber indices and values as the number of nonzeros in the corresponding slice or fiber. One main difference of the hash-based method from other methods in FEATEN is that it does not follow the mode-order approach, rather it extracts the slice and fiber features independently.

Sorting-based method: Another approach for feature extraction is based on sorting the tensor. It is the conventional approach for extracting the features or constructing compressed storage formats for tensors in the literature [21, 29, 33]. It naturally follows the mode-order approach by sorting the tensor indices according to a given mode-order. After sorting, the array construction phase becomes easier since the nonzeros belonging to the same fiber or slice are positioned consecutively. The related work [33] assumes the tensor to be given as sorted and computes the features only for a single mode-order. However, this assumption is not valid when it comes to executing in the upcoming mode-orders. In other words, a tensor \mathcal{X} sorted in $\langle 1, 2, 3 \rangle$ order has to be re-sorted for $\langle 2, 3, 1 \rangle$ and $\langle 3, 1, 2 \rangle$ orders to execute the features for other modes. Instead, we find the tensor features along all modes by sorting the related indices of tensor.

Grouping-based method: Instead of sorting the tensor nonzeros fully, we group the slices and fibers according to their indices and keep the last indices of the COO format in their original order. We first find the number of nonzero fibers and slices by traversing the tensor entries. We store the indices of these nonzero slices and fibers in a compressed manner and track their nonzero counts in the respective arrays. This algorithm takes inspiration from the construction process of Compressed Sparse Row and Column (CSR and CSC) formats for sparse matrices.

Algorithm 1 shows the pseudo-code of the grouping-based feature extraction method for the mode-order $\langle 1, 2, 3 \rangle$ of a 3-mode tensor. In this case, the algorithm considers mode-(2,3) slices and mode-3 fibers. *cnt1* is a temporary array that keeps the nonzero count information for all slices (Lines 1-4). It is used to obtain the number of nonzero slices (n_{slc}), the array of nonzero counts for each nonzero slice (n_{slc}^{nz}), the array of indices for nonzero slices (ind_{slc}), and the array of starting locations for nonzero slices ((xn_{slc}^{nz})) that is similar to the *row_ptr* array in CSR format for matrices (Lines 5-8). *loc* and *order* are temporary arrays that are constructed (Lines 10-16) to obtain the *cnt2* array, which keeps the nonzero count information for all fibers in each nonzero slice (Lines 18-21). Finally, *cnt2* is used to obtain the number of nonzero fibers (n_{slc}^{fib}) and the array of nonzero counts per nonzero fiber (n_{fib}^{nz}) in each nonzero slice (Lines 22-23).

The memory requirement of this algorithm is $I_1 + I_2 + NNZ$ for executing the $(i_1, i_2, :)$ fibers of an $I_1 \times I_2 \times I_3$ tensor with NNZ nonzeros. The worst case serial runtime is $O(I_1 + I_2 S_1)$ where S_1 is the number of nonzero slices in mode 1. For the general case, $size(m) \times size(m + 1)$ is a loose upper bound for mode m .

Algorithm 1 Grouping-Based Extraction Method in FEATEN

Input: 3-mode tensor with COO-arrays $\mathcal{X}_1, \mathcal{X}_2, \mathcal{X}_3$
Output: $n_{slc}^{nz}, n_{fib}^{nz}, n_{slc}^{fib}$ arrays for mode-order $\langle 1, 2, 3 \rangle$

- 1: Create the array $cnt1$ of size I_1 and initialize to zero
- 2: **for** $i \leftarrow 0$ to NNZ **do**
- 3: $cnt1(\mathcal{X}_1(i)) ++$ ▷ Temporary array for nonzeros per slices
- 4: **end for**
- 5: $nslc \leftarrow \# \text{ nz values in } cnt1$ ▷ Number of nonzero slices
- 6: $n_{slc}^{nz} \leftarrow \text{nz values in } cnt1 \text{ (size } I_1)$ ▷ Number of nonzeros per nonzero slice
- 7: $ind_{slc} \leftarrow \text{indices of nz values in } cnt1 \text{ (size } I_1)$
- 8: $xn_{slc}^{nz} \leftarrow \text{PrefixSum}(n_{slc}^{nz})$
- 9: Create the array loc of size $ind_{slc}(I_1)+1$
- 10: **for** $i \leftarrow 0$ to $nslc$ **do**
- 11: $loc(ind_{slc}^{nz}(i)) \leftarrow xn_{slc}^{nz}(i)$
- 12: **end for**
- 13: Create the array $order$ of size NNZ
- 14: **for** $i \leftarrow 0$ to NNZ **do**
- 15: $order(loc(\mathcal{X}_1(k)) ++) \leftarrow k$
- 16: **end for**
- 17: **for** $i \leftarrow 0$ to $nslc$ **do**
- 18: Create the array $cnt2$ of size I_2 and initialize to zero ▷ Temporary array for nonzeros per fiber
- 19: **for** $j \leftarrow xn_{slc}^{nz}(i)$ to $xn_{slc}^{nz}(i+1)$ **do**
- 20: $cnt2(\mathcal{X}_2(order(j))) ++$
- 21: **end for**
- 22: $n_{slc}^{fib}(i) \leftarrow \# \text{ nz in } cnt2$ ▷ Number of nonzero fibers per nonzero slice
- 23: $n_{fib}^{nz}(i) \leftarrow \text{nz values in } cnt2 \text{ (size } n_{slc}^{fib}(i))$ ▷ Number of nonzeros per nonzero fiber
- 24: **end for**

Hybrid method: We propose a hybrid method by combining the sorting- and grouping-based methods. The idea is to utilize different methods for extracting features in different modes within the same tensor. This is because the performance of different methods varies depending on the size of the respective mode. Since we observe that sorting- and grouping-based methods are the best-performing ones at the mode level, we use them interchangeably according to the respective mode size. For mode m , we apply the grouping-based method if $size(m) \times size(m+1) < 10^9$ holds, and we apply the sorting-based method otherwise.

3.4 Extension to Higher Orders

Hash-based method is the only method in FEATEN that does not follow the mode-order approach. Despite its slight disadvantage for the 3-mode case, this difference makes it more applicable for higher-order tensors due to the increased gap between the number of slice-modes and fiber-modes. Additionally, the vast number of features required for extracting higher-order tensors complicates the evaluation process. For these reasons, we only allow the hash-based method to extract all features along all modes for tensors with an order higher than 3. For other methods in FEATEN, we opt to extract the features along the modes with the three largest sizes. For this, we simply sort the tensor modes according to their sizes, select the three largest ones, and extract the features corresponding solely to those modes. We

refer to it as the *only-3-mode* option, which is also available for the hash-based method, in addition to the choice to extract features along all M modes.

4 SPARSE TENSOR GENERATOR

Despite the increased need for research in sparse tensors, publicly available sparse tensor datasets remain limited, comprising only a few instances [12, 28]. To address this scarcity and facilitate the study of machine learning models with a larger variety of sparse tensors, as well as to expand the size of open datasets, we introduce a smart sparse tensor generator, called GENTEN. This generator also enables rapid evaluation of proposed methods and algorithms without the necessity of storing the tensor.

4.1 Overview

Our generator considers the significant features of tensors. Consequently, the artificial tensors produced by GENTEN closely emulate real tensors with their respective features and characteristics. A notable advantage of this developed generator is its utilization of size-independent features, such as coefficient of variation, imbalance, and density. This allows for easy generation of instances with varying sizes, enhancing its versatility and applicability in diverse contexts.

In GENTEN, we provide the option to get the seed for pseudo-randomness from the user. Through this, one can obtain the exact same tensor when providing the same seed in different tests. Moreover, the user can create tensors with almost the same properties by simply changing the seed. The effect of seed selection will be discussed in Section 5.3.3. All levels of GENTEN are parallelized using OpenMP for faster execution.

The main idea of the proposed tensor generator is to first determine fiber counts per slice, and the number of nonzeros per fiber according to the given coefficient of variation values. The generator has the flexibility to employ any distribution to determine these counts, yet we are currently utilizing normal or log-normal distributions to determine the nonzero layout. The positions of the nonzeros and nonzero slice or fiber indices are selected uniformly. The nonzero values are selected uniformly from the interval (0,1).

The generator is general and can generate any M -mode tensor. For ease of expression, we describe the algorithm for a 3-mode tensor. Since generating random sparse tensors while simultaneously adhering to features along all modes is nearly impossible, we opt to consider the features of mode-(2, 3) slices and mode-2 fibers as inputs.

4.2 The Proposed Algorithm

The pseudocode of the proposed sparse tensor generator (GENTEN) is shown in Algorithm 2. The generator utilizes a set of given metrics to create a tensor having these features: (i) sizes of the tensor I_1, I_2, I_3 , (ii) densities of slices, fibers, and nonzeros d^{slc}, d^{fib}, d^{nz} , (iii) coefficient of variations for fibers per slice and nonzeros per fiber $cv_{slc}^{fib}, cv_{fib}^{nz}$, and (iv) imbalance for fibers per slice and nonzeros per fiber $imbal_{slc}^{fib}, imbal_{fib}^{nz}$.

The algorithm first calculates the requested nonzero slice count ($nslc$), and the average, standard deviation, and maximum values for fibers per slice ($avg_{slc}^{fib}, stDev_{slc}^{fib}, max_{slc}^{fib}$) from the given inputs. In line 2, the nonzero slice indices are determined by the RandInds function, which returns $nslc$ many different indices uniformly distributed in the interval $[1, I_1]$. In line 3, the number of fibers per slice (n_{slc}^{fib}) array is constructed and the indices of these nonzero fibers (ind_{fib}) are determined respecting the $avg_{slc}^{fib}, stDev_{slc}^{fib}$, and max_{slc}^{fib} values, using the function Distribute. The details of the Distribute method will be discussed later. A simple prefix sum is applied on n_{slc}^{fib} and we obtain xn_{slc}^{fib} , to be mainly used in future calculations; yet the number of nonzero fibers ($nfib$) is derived by using xn_{slc}^{fib} (Lines 4-5).

Algorithm 2 GENTEN: Sparse Tensor Generator

Input: $I_1, I_2, I_3, d^{slc}, d^{fib}, d^{nz}, cv_{slc}^{fib}, cv_{fib}^{nz}, imbal_{slc}^{fib}, imbal_{fib}^{nz}$
Output: Tensor \mathcal{X} stored in COO format

```

1: Calculate  $nslc, avg_{slc}^{fib}, stDev_{slc}^{fib}, max_{slc}^{fib}$ 
2:  $ind_{slc} \leftarrow \text{RandInds}(nslc, I_1)$  ▷ Array of nonzero slice indices
3:  $(n_{slc}^{fib}, ind_{fib}) \leftarrow \text{Distribute}(nslc, avg_{slc}^{fib}, stDev_{slc}^{fib}, max_{slc}^{fib}, I_2)$  ▷ Number and indices of fibers per slice
4:  $xn_{slc}^{fib} \leftarrow \text{PrefixSum}(n_{slc}^{fib})$ 
5:  $nfib \leftarrow xn_{slc}^{fib}(nslc)$  ▷ Number of nonzero fibers
6: Calculate  $avg_{fib}^{nz}, stDev_{fib}^{nz}, max_{fib}^{nz}$ 
7:  $(n_{fib}^{nz}, ind_{nz}) \leftarrow \text{Distribute}(nfib, avg_{fib}^{nz}, stDev_{fib}^{nz}, max_{fib}^{nz}, I_3)$  ▷ Number and indices of nonzeros per fiber
8:  $xn_{fib}^{nz} \leftarrow \text{PrefixSum}(n_{fib}^{nz})$ 
9: for  $i \leftarrow 0$  to  $nslc$  do
10:   for  $j \leftarrow 0$  to  $n_{slc}^{fib}(i)$  do
11:      $j' \leftarrow xn_{slc}^{fib}(i) + j$  ▷ Global nonzero fiber index
12:     for  $k \leftarrow 0$  to  $n_{fib}^{nz}(j')$  do
13:        $k' \leftarrow xn_{fib}^{nz}(j') + k$  ▷ Global nonzero index
14:        $\mathcal{X}(k') \leftarrow \langle ind_{slc}(i), ind_{fib}(i)(j), ind_{nz}(j')(k) \rangle$  ▷ Fill nonzeros of tensor  $\mathcal{X}$ 
15:     end for
16:   end for
17: end for

```

We calculate the average, standard deviation, and maximum values for nonzeros per fiber ($avg_{fib}^{nz}, stDev_{fib}^{nz}, max_{fib}^{nz}$) according to the determined $nfib$ value. In line 7, the number of nonzeros per fiber (n_{fib}^{nz}) array is constructed and the indices of these nonzeros (ind_{nz}) are determined respecting the $avg_{fib}^{nz}, stDev_{fib}^{nz}, max_{fib}^{nz}$ values, again using the Distribute method. Similarly, the array xn_{fib}^{nz} is obtained by applying prefix sum on n_{fib}^{nz} (Line 8). In the last stage of the algorithm (Lines 9-17), the indices of tensor \mathcal{X} are filled using the arrays ind_{slc} , ind_{fib} , and ind_{nz} .

The pseudocode of the Distribute method is given in Algorithm 3. This method takes five values as inputs, then returns a count array cnt and an index array $inds$. We utilize the Box-Muller method [9] which generates random numbers with normal distribution obeying a given standard deviation and mean. Since this method obeys a continuous distribution, the values are real and sometimes might be negative. However, our aim here is to construct a count array, e.g. keeping track of the nonzero count in nonzero fibers, so the target values should be positive integers. Thus we round the generated values to the nearest positive integers. To avoid negative values, we switch to the log-normal distribution when needed, which guarantees positive real values.

The algorithm applies normal distribution if most values are expected to be positive ($avg - 3 \times std > 0$), or log-normal distribution, otherwise (Lines 1-8). This choice stems from the fact that approximately 99.7% of values sampled from a normal distribution fall within three standard deviations of the mean. Then the algorithm scales the values of cnt if the ratio of the resulting over the expected average is outside of a predetermined range, which is determined as (0.95, 1.05) in our case (Lines 10-16). Finally in Lines 17-21, the values of cnt are adjusted to obey the minimum and maximum values, and the indices are selected uniformly using the RandInds method, which returns $cnt(i)$ many indices in the interval $[1, limit]$.

Algorithm 3 Distribute**Input:** Values $n, avg, std, max, limit$ **Output:** Arrays cnt and $inds$

```

1: for  $i \leftarrow 0$  to  $n$  do
2:   if  $avg > 3 \times std$  then                                     ▷ Apply normal distribution
3:      $cnt(i) \leftarrow \text{BoxMuller}(avg, std)$ 
4:   else                                                         ▷ Apply log-normal distribution
5:      $avg_{logNorm} \leftarrow \log(avg^2 / (avg^2 + std^2)^{1/2})$ 
6:      $std_{logNorm} \leftarrow (\log(1 + std^2 / avg^2))^{1/2}$ 
7:      $cnt(i) \leftarrow \exp(\text{BoxMuller}(avg_{logNorm}, std_{logNorm}))$ 
8:   end if
9: end for
10:  $avg_{result} \leftarrow \text{sum}(cnt) / n$ 
11:  $ratio = avg / avg_{result}$ 
12: if  $ratio < 0.95$  or  $ratio > 1.05$  then                             ▷ Apply scaling if needed
13:   for  $i \leftarrow 0$  to  $n$  do
14:      $cnt(i) \leftarrow cnt(i) \times ratio$ 
15:   end for
16: end if
17: for  $i \leftarrow 0$  to  $n$  do
18:    $cnt(i) \leftarrow \min(cnt(i), max)$ 
19:    $cnt(i) \leftarrow \max(cnt(i), 1)$ 
20:    $ind(i) \leftarrow \text{RandInds}(cnt(i), limit)$                      ▷ Array of size  $cnt(i)$ , with elements in range  $[1, limit]$ 
21: end for

```

4.3 Extension to Higher Orders

The algorithm of GENTEN for higher orders is similar to the one for the 3rd-order case with the main lines. For an M -mode tensor, we consider the features of mode- $(M-1, M)$ slices and mode- $(M-1)$ fibers as inputs. The primary additional challenge in a higher-order setting is determining the indices of nonzero slices. It is because for an M -mode tensor, the nonzero slice indices themselves form a $(M-2)$ -mode smaller boolean tensor, while they were simply scalars for a 3-mode tensor. Therefore we propose a different scheme to determine the indices of nonzero slices efficiently.

We consider four distinct cases regarding the given slice density, d^{slc} , which is the ratio of nonzero slice count ($nslc_{nz}$) over the total slice count ($nslc_{all}$). If $d^{slc} > 0.97$, we round it to 1.0 and assign the slice indices in sorted order. If $d^{slc} \in (0.5, 0.97]$, we create an array of size $nslc_{all}$ to keep track of empty slice indices with the assumption that it can fit into memory, since $nslc_{all}$ can be at most 2 times larger than $nslc_{nz}$. If $d^{slc} \in [0.1, 0.5]$, instead of creating such an array, we traverse all possible $nslc_{all}$ indices and select a fraction of d^{slc} of these indices uniformly. Finally if $d^{slc} < 0.1$, we simply generate $nslc_{nz}$ many random indices for each of the respective $(M-2)$ modes.

5 EVALUATION**5.1 Experimental setup**

The experiments are conducted on an AMD EPYC 7352 CPU of 3200MHz with 512 GB of memory. It has Zen 2 microarchitecture, which includes 2 sockets, and each socket has 24 cores with 2-way simultaneous multi-threading. Both tools are implemented in C/C++ utilizing OpenMP for shared memory parallelism and compiled with GCC using optimization level O2.

Table 3. Properties of the real sparse tensors from the FROSTT and HaTeN2 collections.

Name	Order	I_1	I_2	I_3	I_4	I_5	Slice Count		Fiber Count		NNZ
							All	Nonzero	All	Nonzero	
LBNL-network	5	1,605	4,198	1,631	4,209	868,131	4.1E+13	1.0E+07	6.9E+16	6.8E+06	1,698,825
NIPS	4	2,482	2,862	14,036	17	-	8.2E+07	3.8E+06	1.0E+11	7.3E+06	3,101,609
uber	4	183	24	1,140	1,717	-	2.6E+06	2.6E+05	4.2E+08	2.8E+06	3,309,490
chicago-crime-comm	4	6,186	24	77	32	-	8.3E+05	7.1E+05	3.1E+07	7.8E+06	5,330,673
chicago-crime-geo	5	6,185	24	380	395	32	1.2E+09	3.0E+07	5.6E+10	2.8E+07	6,327,013
vast-2015-mc1-3d	3	165,427	11,374	2	-	-	1.8E+05	1.8E+05	1.9E+09	2.6E+07	26,021,854
vast-2015-mc1-5d	5	165,427	11,374	2	100	89	3.6E+11	1.2E+08	1.7E+13	1.0E+08	26,021,945
DARPA1998	3	22,476	22,476	23,776,223	-	-	2.4E+07	2.4E+07	1.1E+12	5.5E+07	28,436,033
enron	4	6,066	5,699	244,268	1,176	-	3.2E+09	2.2E+07	1.2E+13	9.0E+07	54,202,099
NELL-2	3	12,092	9,184	28,818	-	-	5.0E+04	5.0E+04	7.2E+08	3.8E+07	76,879,419
freebase_music	3	23,343,790	23,344,784	166	-	-	4.7E+07	4.6E+07	5.4E+14	2.2E+08	99,546,551
flickr-3d	3	319,686	28,153,045	1,607,191	-	-	3.0E+07	3.0E+07	5.5E+13	1.5E+08	112,890,310
flickr-4d	4	319,686	28,153,045	1,607,191	731	-	5.5E+13	1.9E+08	1.5E+19	2.8E+08	112,890,310
freebase_sampled	3	38,954,435	38,955,429	532	-	-	7.8E+07	7.4E+07	1.5E+15	3.2E+08	139,920,771
delicious-3d	3	532,924	17,262,471	2,480,308	-	-	2.0E+07	2.0E+07	5.3E+13	1.6E+08	140,126,181
delicious-4d	4	532,924	17,262,471	2,480,308	1,443	-	5.3E+13	2.3E+08	4.4E+18	4.0E+08	140,126,220
NELL-1	3	2,902,330	2,143,368	25,495,389	-	-	3.1E+07	3.1E+07	1.3E+14	2.5E+08	143,599,552

The dataset is taken from two real-world sparse tensor collections, namely FROSTT [28] and HaTen2 [12]. We have excluded the tensors whose nonzero count is more than 1 billion. We have also excluded the delicious-4d tensor since its fiber count exceeds the maximum value (1.8×10^{19}) for an unsigned long long int in the C language. As a result, the dataset consists of 16 real-world sparse tensors whose properties are given in Table 3.

5.2 Performance of Feature Extraction Methods

The performance of four different feature extraction methods in FEATEN are compared. For this experiment, we use the maximum number of available hardware threads in the machine, which is 96. Since all feature extraction methods give the same and exact results as feature sets, we do not present an accuracy comparison among them. Since our dataset includes both 3rd order and higher order tensors, for a fair comparison, we run all four methods in FEATEN with the only-3-mode option, i.e. we extract the features corresponding to modes with the largest three sizes.

Figure 3 shows the total feature extraction time for each method and each tensor. The tensors are shown in increasing order of nonzero counts. Excluding the hybrid method, we observe that the grouping-based method is superior for smaller tensors, whereas the sort-based method is better for larger tensors. Overall, the hybrid method is the best-performing one for all cases except some small tensors, for which the grouping-based method is the best.

A more detailed mode-level comparison of the sorting- and grouping-based methods is given in Table 4. It is seen that the superiority of a method varies between different modes within the execution of each tensor. Although the grouping-based method tends to be costly in total time due to some modes with larger sizes, it is still the winner for some modes of even large tensors. This is the main reason why integrating the grouping-based method for specific modes within the hybrid approach yields improved performance.

5.3 Performance of Tensor Generator

We evaluate the effectiveness of the proposed tensor generator in terms of feature quality, tensor decomposition performance, and sensitivity to seed selection. The generated tensors are created by GENTEN using the features of

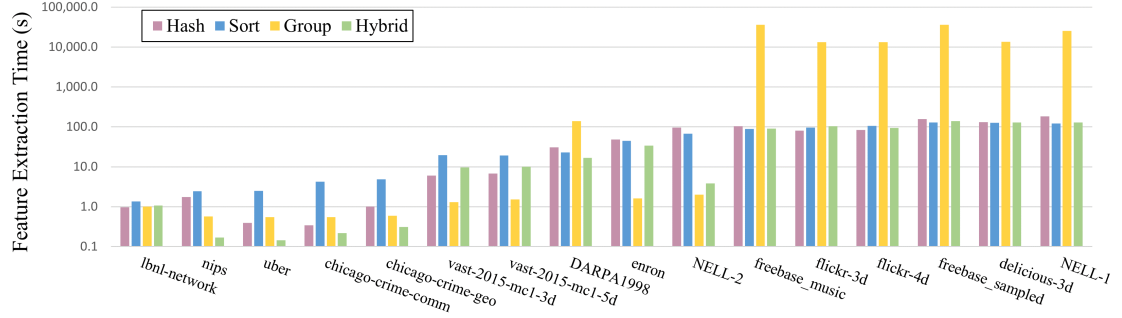


Fig. 3. Runtime comparison for different feature extraction methods.

Table 4. Comparison of sort- and group-based methods in terms of mode-level runtime in seconds. Best results for each mode are shown in bold.

Tensor	Sort-based			Group-based		
	mode-1	mode-2	mode-3	mode-1	mode-2	mode-3
lbnl-network	0.6	0.4	0.3	0.3	0.6	0.6
nips	1.0	0.7	0.7	0.1	0.1	0.2
uber	1.1	0.7	0.7	0.1	0.1	0.1
chicago-crime-comm	1.8	1.2	1.2	0.1	0.1	0.1
chicago-crime-geo	2.1	1.3	1.3	0.2	0.2	0.2
vast-2015-mc1-3d	8.3	5.7	5.2	0.6	0.8	0.9
vast-2015-mc1-5d	8.0	5.4	5.4	0.8	0.8	1.0
DARPA1998	8.9	6.2	6.7	1.3	103.1	138.0
enron	16.7	14.6	12.4	0.7	0.8	1.2
NELL-2	26.0	20.8	19.1	0.8	0.9	1.5
freebase_music	34.4	28.6	22.0	3.4	16.7	36,000.0
flickr-3d	38.2	29.8	24.6	318.7	4,846.7	13,158.4
flickr-4d	38.9	39.1	24.4	326.7	4,798.0	13,109.2
freebase_sampled	50.6	42.6	32.0	8.3	28.4	36,000.0
delicious-3d	51.1	39.6	31.4	1,209.3	4,840.3	13,517.2
NELL-1	47.4	38.3	33.0	4,346.7	21,478.6	25,526.0

real tensors, which are obtained via our feature extractor FEATEN. Except for the sensitivity analysis part, we use the generated tensors in which the seed for pseudo-randomness is set to 0.

5.3.1 Feature Quality. Table 5 shows the comparison of the generated tensors with their original versions, i.e. real tensors, in terms of some important features. We present the features of the original and the respective generated tensors, as well as the ratio of the resulting value of the generated tensor over that of the original tensor. The ratio values are colored green if the value is between 0.9 and 1.1; red if it is less than 0.5 or more than 2; and orange, otherwise. For zero or too small (less than 0.1) coefficient of variation values, the generator often yields values with zero coefficient of variation. For those cases, the ratio values are omitted from the table since the ratio will appear as either zero or undefined (0/0).

As can be seen in the table, the resulting densities, i.e. the nonzero count of the generated tensors, are at least 0.96 times smaller or at most 1.05 times larger than the ones of the respective original tensors. The success of the generator in terms of obeying the given density is seen in both levels of nonzero slice, nonzero fiber, and nonzero density.

Table 5. Feature comparison of the generated tensors with their original versions; and time to generate tensors.

Name	Coefficient of Variation						Density									Time (s)
	Fiber per Slice			Nonzero per Fiber			Nonzero Slice			Nonzero Fiber			Nonzero			
	Org	Gen	Ratio	Org	Gen	Ratio	Org	Gen	Ratio	Org	Gen	Ratio	Org	Gen	Ratio	
LBNL-network	8.0	4.5	0.56	26.2	12.1	0.46	2.1E-06	2.1E-06	1.00	8.4E-10	9.5E-10	1.13	4.2E-14	4.4E-14	1.05	1.0
NIPS	0.2	0.2	0.98	0.0	0.0	-	8.3E-04	8.3E-04	1.00	3.1E-05	3.0E-05	0.98	1.8E-06	1.8E-06	0.98	0.3
uber	0.2	0.2	0.94	1.0	1.0	0.94	1.0E+00	1.0E+00	1.00	1.4E-01	1.3E-01	0.93	3.8E-04	3.8E-04	0.99	0.1
chicago-crime-comm	0.4	0.3	0.82	0.5	0.4	0.82	9.5E-01	9.5E-01	1.00	3.2E-01	2.7E-01	0.83	1.5E-02	1.4E-02	0.96	0.3
chicago-crime-geo	0.3	0.3	0.94	0.1	0.0	-	1.0E-01	1.0E-01	1.00	2.8E-04	2.9E-04	1.01	8.9E-06	8.9E-06	1.01	1.6
vast-2015-mc1-3d	0.5	0.5	1.00	0.0	0.0	-	1.0E+00	1.0E+00	1.00	1.4E-02	1.4E-02	0.99	6.9E-03	6.9E-03	0.99	2.2
vast-2015-mc1-5d	0.0	0.0	-	0.0	0.0	-	6.9E-03	6.9E-03	1.00	6.9E-05	6.9E-05	1.00	7.8E-07	7.8E-07	1.00	4.8
DARPA1998	13.1	8.2	0.63	23.1	14.0	0.61	8.0E-01	8.1E-01	1.02	1.5E-04	1.6E-04	1.03	2.4E-09	2.4E-09	1.00	147.8
enron	4.1	3.6	0.87	1.8	1.4	0.76	4.4E-03	4.4E-03	1.00	3.7E-06	3.7E-06	0.99	5.5E-09	5.7E-09	1.05	3.1
NELL-2	3.3	3.1	0.94	0.9	1.1	1.25	1.0E+00	1.0E+00	1.00	3.0E-03	3.1E-03	1.01	2.4E-05	2.4E-05	0.99	0.6
freebase_music	24.4	20.2	0.83	0.1	0.0	-	9.7E-01	1.0E+00	1.03	1.8E-07	1.9E-07	1.04	1.1E-09	1.1E-09	1.03	4,370.6
flickr-3d	3.3	3.2	0.97	1.0	1.0	0.99	1.0E+00	1.0E+00	1.00	3.1E-06	3.1E-06	1.00	7.8E-12	7.9E-12	1.01	2,080.4
flickr-4d	1.0	1.0	0.99	0.0	0.0	-	3.1E-06	3.1E-06	1.00	7.8E-12	7.9E-12	1.01	1.1E-14	1.1E-14	1.01	1,180.8
freebase_sampled	24.0	19.4	0.81	0.1	0.0	-	9.1E-01	9.1E-01	1.00	9.2E-08	9.6E-08	1.05	1.7E-10	1.8E-10	1.04	10,608.6
delicious-3d	2.8	2.7	0.99	1.4	1.0	0.71	1.0E+00	1.0E+00	1.00	5.1E-06	5.1E-06	1.00	6.1E-12	6.1E-12	1.00	6,332.0
NELL-1	13.6	10.8	0.80	7.5	4.5	0.60	1.0E+00	1.0E+00	1.00	2.8E-06	2.8E-06	1.01	9.1E-13	9.2E-13	1.01	23,384.5

In methods that generate values to obey a given density and variation, there is a trade-off between strictly obeying the density or the variation. In other words, if one prioritizes achieving the exact coefficient of variation, the density might get far from the desired value. However, since the number of nonzeros is the most significant feature that a generator must obey for performance concerns, we opted to prioritize adhering to density. For this, in GENTEN we apply some scalings during calculations to catch the given density. It is the reason why the resulting ratios in coefficient of variation seem relatively low compared to the ratios in densities.

We also present the tensor generation times in the last column of Table 5. These are the runtime of GENTEN in seconds when working with the maximum available thread count, which is 96 in our case. We observe that GENTEN takes only a few seconds when generating medium-size tensors. To be precise, it takes less than 5 seconds for 9 out of 16 tensors. Only for some large tensors (4 cases in our dataset), the runtime of GENTEN can go up to a few hours. Note that the execution of GENTEN depends on the requested nonzero count as well as the slice and fiber counts; thus the sizes of the tensor also affect the execution time.

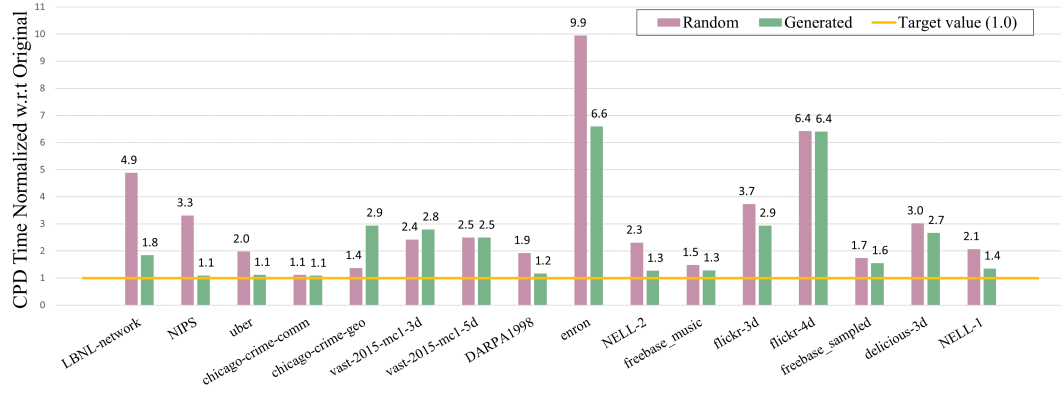
5.3.2 CPD Performance. We evaluate the effectiveness of the generated tensors in mimicking the behavior of real tensors, particularly in terms of tensor decomposition performance. For this, the performance of the generated tensors is compared with the performance of the naive random tensors, which have the same sizes and nonzero counts as the original tensors but the nonzero locations are uniformly random. The SPLATT [31] and ParTI [20] tools are used for applying the CPD decomposition for 50 iterations, by ignoring the first 5 iterations for a warm cache. For each case, we take 5 independent runs and choose the minimum runtime to represent the peak performance of the system and to be less susceptible to noise than the average.

Figure 4 illustrates the comparison between the generated and naive random tensors in their ability to resemble real tensors regarding the CPD performance. The runtime results for both the naive random and the generated tensors are normalized with respect to the runtime obtained for the respective original tensor. Therefore, the normalized values closer to 1.0 are interpreted as more successful in terms of resembling the original tensor performance.

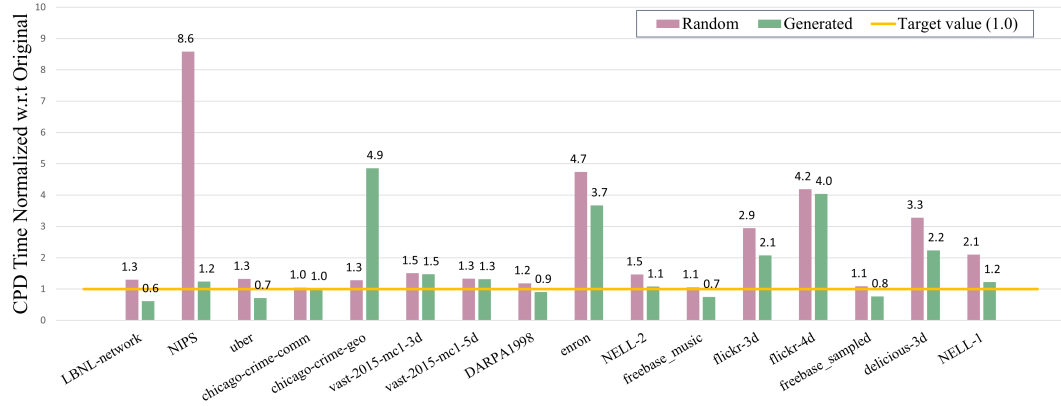
Figure 4a depicts the CPD performance comparison by using the ParTI tool with a single thread. It is evident that the generated tensors emerge as the clear winner in most cases, and in the remaining scenarios, they are comparable to



(a) ParTI performance comparison for a single thread



(b) SPLATT performance comparison for a single thread



(c) SPLATT performance comparison for 48 threads

Fig. 4. CPD performance comparison of the naive random and the generated tensors. The values are normalized with respect to the runtime obtained for the respective original tensor.

Table 6. Comparison of the generated tensors with different seeds in terms of nonzero count and CPD time in seconds.

Name	Nonzero Count				CPD Time (1 Thread)				CPD Time (48 Threads)			
	Seed=0	Seed=1	Seed=2	CV	Seed=0	Seed=1	Seed=2	CV	Seed=0	Seed=1	Seed=2	CV
LBNL-network	1,699,088	1,699,162	1,699,444	9.0E-05	21.3	21.3	22.1	1.8E-02	3.9	5.0	4.9	1.1E-01
NIPS	3,041,941	3,042,054	3,041,816	3.2E-05	6.1	6.1	6.7	3.9E-02	0.5	0.5	0.6	4.2E-02
uber	3,283,106	3,282,919	3,283,336	5.2E-05	6.4	6.3	6.3	6.1E-03	0.3	0.3	0.3	0.0E+00
chicago-crime-comm	5,131,130	5,131,402	5,131,234	2.2E-05	8.0	7.7	7.9	1.5E-02	0.4	0.4	0.4	7.0E-03
chicago-crime-geo	6,364,282	6,364,306	6,365,068	5.7E-05	75.3	100.8	90.9	1.2E-01	7.9	9.8	8.8	8.9E-02
vast-2015-mc1-3d	25,800,284	25,802,581	25,801,506	3.6E-05	64.1	67.1	70.4	3.8E-02	29.1	31.3	29.7	3.1E-02
vast-2015-mc1-5d	26,021,841	26,021,841	26,021,841	0.0E+00	268.9	269.6	268.9	1.2E-03	218.4	214.2	212.2	1.2E-02
DARPA1998	28,732,452	28,406,813	28,405,526	5.4E-03	250.7	251.5	269.8	3.4E-02	84.6	94.6	93.0	4.8E-02
enron	56,967,347	57,055,466	57,032,145	6.5E-04	588.9	670.4	651.7	5.5E-02	29.8	32.7	32.7	4.3E-02
NELL-2	76,203,551	76,202,209	76,203,884	9.5E-06	89.8	89.5	90.1	2.6E-03	7.7	7.9	7.8	1.4E-02
freebase_music	102,877,680	102,916,007	102,874,661	1.8E-04	1,459.2	1,495.5	1,480.7	1.0E-02	243.3	316.4	312.1	1.2E-01
flickr-3d	113,727,282	113,736,842	113,674,701	2.4E-04	1,471.7	1,458.7	1,544.7	2.5E-02	261.1	292.3	308.5	6.8E-02
flickr-4d	113,641,027	113,641,445	113,640,707	2.7E-06	4,714.5	4,786.8	4,700.2	8.0E-03	596.7	579.3	627.7	3.3E-02
freebase_sampled	145,748,228	145,801,470	145,741,097	1.8E-04	2,409.9	2,424.5	2,493.8	1.5E-02	380.6	465.8	482.4	1.0E-01
delicious-3d	139,996,876	139,993,400	139,999,596	1.8E-05	1,845.9	1,835.4	1,833.6	3.0E-03	290.3	350.6	328.5	7.7E-02
NELL-1	145,175,629	145,155,883	145,155,081	6.5E-05	1,513.9	1,599.3	1,609.8	2.7E-02	256.0	300.6	292.8	6.9E-02

the naive random tensors but never inferior. The superiority of the generated tensors over the naive random ones is especially higher for larger tensors. The ParTI tool gave an error for the chicago-crime-geo tensor, so this tensor is not presented in Figure 4a and the rest of the experiments are conducted by using only the SPLATT tool.

In Figure 4b, we present the CPD performance comparison by using the SPLATT tool with a single thread. As seen in the figure, the generated tensors show significantly better performance than the naive random ones for 11 out of 16 cases; and yield similar performance with naive random tensors for 3 tensors in the serial setting. For instance, for the NIPS tensor, while the naive random tensor is 3.3 times slower than the original tensor, the tensor generated with GENTen yields a CPD time of only 1.1 times more than the runtime of the original real tensor.

Figure 4c shows the CPD performance comparison by using SPLATT with 48 threads. We observe that the generated tensors are superior to the naive random ones for 8 cases; and inferior for only 1 tensor (chicago-crime-geo). The generated tensors show almost the same performance as the naive random ones for 3 cases but for those, their performance is either already the same as the respective real tensor (chicago-crime-comm), or only 1.3 (vast-2015-mc1-5d) and 1.5 (vast-2015-mc1-3d) times far from the performance of the original tensors.

5.3.3 Sensitivity Analysis. To evaluate the sensitivity of our generator, we produce 3 different versions for each generated tensor by taking the seed for pseudo-randomness as 0, 1, and 2. Table 6 shows the nonzero counts and the CPD (SPLATT) runtime for 1 and 48 threads (in seconds). We present the coefficient of variation (CV) for each case. As can be seen in the table, the CV for nonzero count is at most 5×10^{-3} , whereas the CV for CPD performance is at most 0.1. That is, the generator is robust in terms of maintaining a consistent sparsity pattern, and the performance of the generated tensor is not highly sensitive to changes in the seed value. It implies that the proposed generator produces reliable and predictable results, providing a dependable tool for generating sparse tensors for various applications.

6 RELATED WORK

To the best of our knowledge, there is only one study (and its extension) that extracts tensor features for optimizing sparse tensor computations in the literature: Sun et al.[32] proposed a framework, namely SpTFS, that automatically predicts the optimal storage format for CPD. SpTFS lowers the sparse tensor to fixed-sized matrices and gives them to

convolutional neural networks (CNN) as inputs along with tensor features. The authors improve SpTFS by adopting both supervised and unsupervised learning-based machine learning models in a recent work [33].

The previous works [32, 33] have considered the features for only one mode, assuming that the tensor is already sorted along that mode. However, real-world tensor sizes diverge significantly so that sizes in some modes reach millions while some are only orders of ten or even less. Therefore, considering the global values might result in losing some important information about the structure of the tensor.

Although several sparse matrix and graph generators are proposed in the literature [4, 6, 17, 23, 24], the studies on sparse tensor generators are very limited. Smith and Karypis [30] used the method of Chi and Kolda [7] to generate synthetic tensors whose values follow a Poisson distribution. Due to the deficiency of publicly available sparse tensors, Sun et al. [32] produced synthetic tensors by combining sparse matrices in Suite Sparse [8] collection such that the elements of matrices form the modes of tensors. Baskaran et al. [5] used MATLAB Tensor Toolkit [15] to generate synthetic sparse tensors but these are rather small tensors with less than one million nonzeros.

7 CONCLUSION

In this study, we introduce two tools, namely FEATEN and GENTEN, that we proposed and developed to facilitate the research in sparse tensor operations. FEATEN is a feature extraction framework for sparse tensors that provides four different methods, with a focus on extracting the tensor features in the most efficient way. This contribution is valuable because even the feature extraction is challenging and costly due to huge fiber and slice counts in real sparse tensors. We provide an evaluation of the performance of different feature extraction methods and observe that the methods whose algorithms are proposed first in this work are preferable to the conventional methods.

GENTEN is a smart sparse tensor generator that obeys a significant and large set of tensor features. The experimental results validate the success of the generator in mimicking the real tensors regarding both sparsity pattern and tensor decomposition performance. GENTEN holds the benefit of utilizing size-independent features so that it can be used to generate tensors with smaller or larger sizes, yet still have similar properties with real tensors. It paves the way for obtaining a large dataset of synthetic sparse tensors that have similar characteristics and behavior with real-world data.

ACKNOWLEDGMENTS

This project has received funding from the European High-Performance Computing Joint Undertaking under grant agreement No 956213. Koç University is supported by the Turkish Science and Technology Research Centre Grant No 120N003.

REFERENCES

- [1] Walid Abu-Sufah and Asma Abdel Karim. 2013. Auto-tuning of sparse matrix-vector multiplication on graphics processors. In *International Supercomputing Conference*. Springer, 151–164.
- [2] Evrim Acar, Canan Aykut-Bingol, Haluk Bingol, Rasmus Bro, and Bülent Yener. 2007. Multiway analysis of epilepsy tensors. *Bioinformatics* 23, 13 (2007), i10–i18.
- [3] Seher Acer, Tugba Torun, and Cevdet Aykanat. 2018. Improving medium-grain partitioning for scalable sparse tensor decomposition. *IEEE Transactions on Parallel and Distributed Systems* 29, 12 (2018), 2814–2825.
- [4] Warren Armstrong and Alistair P Rendell. 2008. Reinforcement learning for automated performance tuning: Initial evaluation for sparse matrix format selection. In *2008 IEEE International Conference on Cluster Computing*. IEEE, 411–420.
- [5] Muthu Baskaran, Benoit Meister, Nicolas Vasilache, and Richard Lethin. 2012. Efficient and scalable computations with sparse tensors. In *2012 IEEE Conference on High Performance Extreme Computing*. IEEE, 1–6.
- [6] Angela Bonifati, Irena Holubová, Arnau Prat-Pérez, and Sherif Sakr. 2020. Graph generators: State of the art and open challenges. *ACM computing surveys (CSUR)* 53, 2 (2020), 1–30.

- [7] Eric C Chi and Tamara G Kolda. 2012. On tensors, sparsity, and nonnegative factorizations. *SIAM J. Matrix Anal. Appl.* 33, 4 (2012), 1272–1299.
- [8] Timothy Davis and Yifan Hu. 2011. The University of Florida Sparse Matrix Collection. *ACM Trans. Math. Software* 38, 1 (2011), 1–25. <https://doi.org/10.1145/2049662.2049663>
- [9] ER Golder and JG Settle. 1976. The Box-Müller Method for Generating Pseudo-Random Normal Deviates. *Journal of the Royal Statistical Society: Series C (Applied Statistics)* 25, 1 (1976), 12–20.
- [10] José Henrique de M Goulart, Maxime Boizard, Rémy Boyer, Gérard Favier, and Pierre Comon. 2015. Tensor CP decomposition with structured factor matrices: Algorithms and performance. *IEEE Journal of Selected Topics in Signal Processing* 10, 4 (2015), 757–769.
- [11] Ahmed E Helal, Jan Laukemann, Fabio Checconi, Jesmin Jahan Tithi, Teresa Ranadive, Fabrizio Petrini, and Jeewhan Choi. 2021. Alto: Adaptive linearized storage of sparse tensors. In *Proceedings of the ACM International Conference on Supercomputing*. 404–416.
- [12] Inah Jeon, Evangelos E Papalexakis, Uksong Kang, and Christos Faloutsos. 2015. Haten2: Billion-scale tensor decompositions. In *2015 IEEE 31st international conference on data engineering*. IEEE, 1047–1058.
- [13] Ante Jukić, Ivica Kopriva, and Andrzej Cichocki. 2013. Noninvasive diagnosis of melanoma with tensor decomposition-based feature extraction from clinical color image. *Biomedical Signal Processing and Control* 8, 6 (2013), 755–763.
- [14] Oguz Kaya and Bora Uçar. 2018. Parallel candecomp/parafac decomposition of sparse tensors using dimension trees. *SIAM Journal on Scientific Computing* 40, 1 (2018), C99–C130.
- [15] Tamara G Kolda and Brett W Bader. 2006. *MATLAB tensor toolbox*. Technical Report. Sandia National Laboratories (SNL), Albuquerque, NM, and Livermore, CA (United States).
- [16] Tamara G Kolda and Brett W Bader. 2009. Tensor decompositions and applications. *SIAM review* 51, 3 (2009), 455–500.
- [17] Tamara G Kolda, Ali Pinar, Todd Plantenga, and Comandur Seshadhri. 2014. A scalable generative graph model with community structure. *SIAM Journal on Scientific Computing* 36, 5 (2014), C424–C452.
- [18] Liwei Kuang, Fei Hao, Laurence T Yang, Man Lin, Changqing Luo, and Geyong Min. 2014. A tensor-based approach for big data representation and dimensionality reduction. *IEEE transactions on emerging topics in computing* 2, 3 (2014), 280–291.
- [19] Éric Leclercq and Marinette Savonnet. 2018. A tensor based data model for polystore: an application to social networks data. In *Proceedings of the 22nd International Database Engineering & Applications Symposium*. 110–118.
- [20] Jiajia Li, Yuchen Ma, and Richard Vuduc. 2018. ParTII: A parallel tensor infrastructure for multicore CPUs and GPUs.
- [21] Jiajia Li, Jimeng Sun, and Richard Vuduc. 2018. HiCOO: Hierarchical storage of sparse tensors. In *SC18: International Conference for High Performance Computing, Networking, Storage and Analysis*. IEEE, 238–252.
- [22] Jiajia Li, Bora Uçar, Ümit V Çatalyürek, Jimeng Sun, Kevin Barker, and Richard Vuduc. 2019. Efficient and effective sparse tensor reordering. In *Proceedings of the ACM International Conference on Supercomputing*. 227–237.
- [23] Piotr Luszczek, Yaohung Tsai, Neil Lindquist, Hartwig Anzt, and Jack Dongarra. 2020. Scalable Data Generation for Evaluating Mixed-Precision Solvers. In *2020 IEEE High Performance Extreme Computing Conference (HPEC)*. IEEE, 1–6.
- [24] Panagiotis Mpakos, Dimitrios Galanopoulos, Petros Anastasiadis, Nikela Papadopoulou, Nectarios Koziris, and Georgios Goumas. 2023. Feature-based spmv performance analysis on contemporary devices. In *2023 IEEE International Parallel and Distributed Processing Symposium (IPDPS)*. IEEE, 668–679.
- [25] Yang Mu, Wei Ding, Melissa Morabito, and Dacheng Tao. 2011. Empirical discriminative tensor analysis for crime forecasting. In *Knowledge Science, Engineering and Management: 5th International Conference, KSEM 2011, Irvine, CA, USA, December 12-14, 2011. Proceedings* 5. Springer, 293–304.
- [26] Israt Nisa, Jiajia Li, Aravind Sukumaran-Rajam, Richard Vuduc, and P Sadayappan. 2019. Load-balanced sparse MTTKRP on GPUs. In *2019 IEEE International Parallel and Distributed Processing Symposium (IPDPS)*. IEEE, 123–133.
- [27] Shruti Shivakumar, Jiajia Li, Ramakrishnan Kannan, and Srinivas Aluru. 2021. Efficient parallel sparse symmetric tucker decomposition for high-order tensors. In *SIAM Conference on Applied and Computational Discrete Algorithms (ACDA21)*. SIAM, 193–204.
- [28] Shaden Smith, Jee W Choi, Jiajia Li, Richard Vuduc, Jongsoo Park, Xing Liu, and George Karypis. 2017. FROSTT: The formidable repository of open sparse tensors and tools.
- [29] Shaden Smith and George Karypis. 2015. Tensor-matrix products with a compressed sparse tensor. In *Proceedings of the 5th Workshop on Irregular Applications: Architectures and Algorithms*. 1–7.
- [30] Shaden Smith and George Karypis. 2017. Accelerating the tucker decomposition with compressed sparse tensors. In *European Conference on Parallel Processing*. Springer, 653–668.
- [31] Shaden Smith, Niranjay Ravindran, Nicholas D Sidiropoulos, and George Karypis. 2015. SPLATT: Efficient and parallel sparse tensor-matrix multiplication. In *2015 IEEE International Parallel and Distributed Processing Symposium*. IEEE, 61–70.
- [32] Qingxiao Sun, Yi Liu, Ming Dun, Hailong Yang, Zhongzhi Luan, Lin Gan, Guangwen Yang, and Depei Qian. 2020. Sptfs: Sparse tensor format selection for mttkrp via deep learning. In *SC20: International Conference for High Performance Computing, Networking, Storage and Analysis*. IEEE, 1–14.
- [33] Qingxiao Sun, Yi Liu, Hailong Yang, Ming Dun, Zhongzhi Luan, Lin Gan, Guangwen Yang, and Depei Qian. 2021. Input-aware Sparse Tensor Storage Format Selection for Optimizing MTTKRP. *IEEE Trans. Comput.* (2021).
- [34] Anil R Yelundur, Vineet Chaoji, and Bamdev Mishra. 2019. Detection of review abuse via semi-supervised binary multi-target tensor decomposition. In *Proceedings of the 25th ACM SIGKDD International Conference on Knowledge Discovery & Data Mining*. 2134–2144.